Energy Engineering

Tech Science Press

DOI: 10.32604/EE.2021.014240

ARTICLE

Scavenging Effects of Kaolin on Fine Ash Formation during Zhundong Coal Combustion

Fangqi Liu[1], Xianpeng Zeng[1,2], Yimin Xia[1], Zihao Wang[1] and Dunxi Yu[1,*]

[1]State Key Laboratory of Coal Combustion, School of Energy and Power Engineering, Huazhong University of Science and Technology, Wuhan, 430074, China

[2]WISDRI Engineering & Research Incorporation Limited, Wuhan, 430223, China

[*]Corresponding Author: Dunxi Yu. Email: dunxiyu@hust.edu.cn

Received: 12 September 2020 Accepted: 18 November 2020

ABSTRACT

The previous work found that the additive kaolin could scavenge not only sodium (Na) but also calcium (Ca) and magnesium (Mg), which is the important ash fluxing agents in low rank coal combustion. Such scavenging effects of kaolin on fine ash formation were studied in the present work. A typical Zhundong coal and its blends with kaolin at dosages of 1, 2 and 4 wt% were combusted in an electrically heated drop tube furnace (DTF) at 1300°C. The fine ashes generated were collected and size segregated by a low pressure impactor (LPI). The morphology and chemical composition of fine ash were analyzed by scanning electron microscopy equipped with an energy-dispersive spectrometer (SEM-EDS). In addition, char/ash particles were sampled at various positions of DTF to elucidate how kaolin additive affected the fine ash formation process. The results further showed that apart from the scavenging of volatile Na, kaolin additive could also strongly scavenge the refractory Ca, Mg and Fe in the fine ash during Zhundong coal combustion, which transformed the sintered particles with irregular shape into melted spherical particles, and finally resulted in the considerable decrease of these elements in both $PM_{0.4}$ and $PM_{0.4\text{-}10}$ by melting and agglomeration. The close contacts between kaolin particles and coal resulted from physically mixing were a key factor responsible for the reaction of kaolin with the refractory Ca, Mg and Fe.

KEYWORDS

Zhundong coal; kaolin; fine ash; basic elements; sodium; ash deposition

1 Introduction

Low rank coals are usually of high content of basic elements (Na, Ca, Mg and/or Fe) [1,2]. These elements were likely to cause troublesome fouling and slagging problems during combustion in boilers, which has long been a problem facing the engineers and scientists in the world [2–8]. Besides, the low rank coals were likely to produce much more fine ash particles (here refer to particles less than 10 μm, PM_{10}) than bituminous coals on the same ash content basis [7,9], which not only contribute to ash deposition but also cause an environmental risk when they were emitted to the atmosphere [10–12]. Extensive research has been conducted on the inorganics transformation, ash formation, deposition and control technologies during low rank coals combustion in the past decades [1,13–18].

In the literature, Na is considered to be the important trigger of ash deposition, as it can easily vaporize from the coal and condense on the surface of boiler tubes, or react with silicates forming sticky particles [5], initiating and accelerating the ash deposition rate. Injection of mineral additives is one of the important control technologies to capture Na vapors [19,20]. In this technology, vapor of Na compounds is captured by the sorbent through chemical reactions and/or physical condensation. Kaolin has been widely studied by many researchers, and found to be the most effective additive in scavenging Na vapor [17,19,21,22], which can subsequently reduce the emissions of Na-containing PM_1 (particulate matter with an aerodynamic diameter less than 1 μm) [23,24] and mitigate the ash deposition [25–27]. Although the mechanisms of reactions between Na and kaolin have been well understood, it is little known whether kaolin additive would also affect other basic elements (such as Ca, Mg and Fe), which are much less volatile than Na. This is of critical importance and needs to be well understood if kaolin is selected as the additive during combustion of low rank coals that are abundant in Ca, Mg or Fe as well as Na. The recent work [28] on a low rank Zhundong coal found that, in addition to Na, the added kaolin could also strongly scavenge refractory elements such as Ca and Mg, forming complex Ca-Mg-Na containing aluminoslicates in the bulk ash. However, the effects of kaolin addition on fine ash particle formation were not discussed. This is particularly investigated in the present work. Two aspects are well addressed: (1) How kaolin addition would affect PM_{10} emissions and particle size distributions; (2) How kaolin addition would affect the partitioning of basic elements such as Na, Ca, Mg and Fe from the coal.

2 Materials and Methods

2.1 Coal and Kaolin Properties

A typical Zhundong coal (denoted as ZD) was studied in this paper, which was the same as the coal used in our previous work [28]. The particle size of the coal sample was less than 100 μm. The proximate and ultimate analysis were performed according to Chinese standards GB/T 30733-2014 and GB/T 476-2008, and are presented in Tab. 1. The low temperature ash of the Zhundong coal was prepared in a low temperature oxygen plasma asher (EMS1050X). Its chemical composition is presented in Tab. 2. Tab. 1 shows that the ash content of Zhundong coal is very low, which is only 3.5 wt%. The contents of Na_2O, MgO and CaO in the low temperature ash (Tab. 2) are 4.86, 6.18 and 33.78 wt%, respectively, which are much higher than typical Chinese coal ashes [29]. The content of Fe_2O_3 is 2.55 wt%, which is at a middle level. While the contents of SiO_2 (9.03 wt%) and Al_2O_3 (8.34 wt%) are much lower than typical Chinese coals. In addition, the content of SO_3 is also high (accounting for 33.96 wt%) due to the sulfation of Na_2O, MgO and CaO during the low temperature ashing process. Our previous work [28] showed that Na was mainly presented as water-soluble form (73 wt%) and organically bond form (24 wt%), while Ca and Mg were mainly in the organically bound form (about 60 wt%). Fe was mainly presented as hydrochloric acid insoluble form (86 wt%), and the rest (14 wt%) was hydrochloric acid soluble, probably as organically bond form [30].

Table 1: Proximate analysis and ultimate analysis of Zhundong coal

Proximate analysis (wt%, ad)				Ultimate analysis (wt%, ad)				
Moisture	Volatile matter	Ash	Fixed carbon	C	H	O*	N	S
6.3	38.2	3.5	52.0	64.9	3.6	18.9	2.4	0.4

* by difference.

The kaolin additive used was the same as that in our previous work [28], which is mainly composed of SiO_2 (60.32 wt%) and Al_2O_3 (37.56 wt%), as shown in Tab. 2. The particle size distribution of kaolin additive was analyzed by a Malvern size analyzer (Mastersizer 2000) and is shown in Fig. 1. The result shows that the mean size of kaolin is about 2.25 μm, and 95% of particles were less than 10 μm.

Table 2: Chemical composition of Zhundong coal low temperature ash and kaolin (wt%)

	Na_2O	MgO	Al_2O_3	SiO_2	P_2O_5	SO_3	K_2O	CaO	Fe_2O_3
Zhundong coal ash	4.86	6.18	8.34	9.03	1.10	33.96	0.20	33.78	2.55
Kaolin	0.38	0.50	37.56	60.32	0.24	0.11	0.26	0.35	0.28

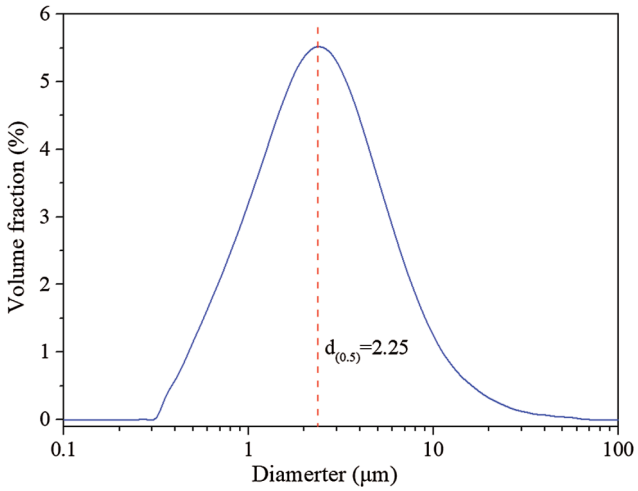

Figure 1: Particle size distribution of kaolin

Kaolin was added to the coal by physically mixing method. The dosages were 1, 2 and 4 wt% of coal mass, which were denoted as ZD + 1% Kaolin, ZD + 2% Kaolin and ZD + 4% Kaolin, respectively.

2.2 Experimental Process and Analysis Methods

The combustion experiments were carried out in a well-controlled electrically heated drop tube furnace. Detailed information on this facility can be found elsewhere [31]. Briefly, the reactor was 2 m long with an inner diameter of 56 mm. The furnace temperature was set at 1300°C. A mixture of O_2/N_2 with a volume ratio of 21/79 was used to simulate air combustion, and the flow rate was 10 L/min. ZD coal and its blends with kaolin were fed at a rate of 0.1 g/min by a microfeeder (model PEF-90A) to the furnace.

After combustion, the particle-loaded flue gas was directed into a water cooled isokinetic sampling probe. A stream of pure N_2 was introduced at the inlet of the probe to dilute and quench the gas, so that further reactions between the fine ash aerosols could be suppressed [32]. Subsequently, the ash particles were collected by a Dekati cyclone and a low pressure impactor (LPI). The cyclone was used to remove particles with an aerodynamic diameter larger than 10 μm. The LPI classified the particles less than 10 μm into 13 fractions. Both the cyclone and LPI were heated to 130°C to avoid the condensation of SO_3, HCl and water vapor [33]. Aluminum foils coated with Apiezon grease (H) were used as substrates for particulate matter collection. The mass of aluminum foils before and after sampling were measured by a high precision (1 μg) balance to obtain the particle mass based size distributions. Meanwhile, Millipore membranes were also used to collect particles for morphology and composition analyses by scanning electron microscopy equipped with an energy-dispersive spectrometer (SEM-EDS, Zeiss Sigma300, Oxford X-MaxN80). In addition to PM_{10}, intermediate char/ash samples were also collected at different positions along the drop tube furnace (0.5, 0.7 and 1 m from the injector) and analyzed. The data were used to elucidate how kaolin additive would affect fine ash formation processes during Zhundong coal combustion.

3 Results

3.1 Fine Ash Particle Size Distributions and Yields before and after Kaolin Addition

The fine ash particle (PM_{10}) size distributions (PSDs) before and after kaolin addition at 1300°C were presented in Figs. 2a and 2b. Generally, in all cases, the PSDs are bimodally distributed in terms of mass. The fine mode was below 0.4 μm (defined as $PM_{0.4}$), with a peak at 0.07 μm. And the coarse mode was in the range of 0.4–10 μm (defined as $PM_{0.4\text{-}10}$), with a peak at 5 μm. According to previous work [11], particles less than 0.1 μm are often called "ultrafine" mode, which is mainly formed by the homogeneous condensation, nucleation and coagulation of vaporized inorganic species. The particles in the range of 0.1–0.4 μm (or larger) is often called the accumulation mode, which is formed by coagulation and heterogeneous condensation of vaporized species. Differently, the coarse mode is mainly formed by the coalescence of included mineral and the fragmentation of char [34]. For ZD coal, the yield of $PM_{0.4}$ was about 0.65 mg/g coal, while the yield of fragmentation mode $PM_{0.4\text{-}10}$ was about 6 mg/g coal, which accounted for 90 wt% of the total PM_{10}. After kaolin addition, the yield of $PM_{0.4}$ was significantly decreased by 40%–50% at the dosages of 1%–4%. While the amount of $PM_{0.4\text{-}10}$ at the same coal input basis was only slightly increased (at 1% and 4% kaolin dosage) or even decreased at 2% kaolin dosage. Considering that kaolin was fine, with the peak size at 2.25 μm (Fig. 1), so it can be speculated that the kaolin additive also interacts with the coarse mode $PM_{0.4\text{-}10}$ from ZD coal. Otherwise, the amount of $PM_{0.4\text{-}10}$ should increase significantly if no interaction has taken place.

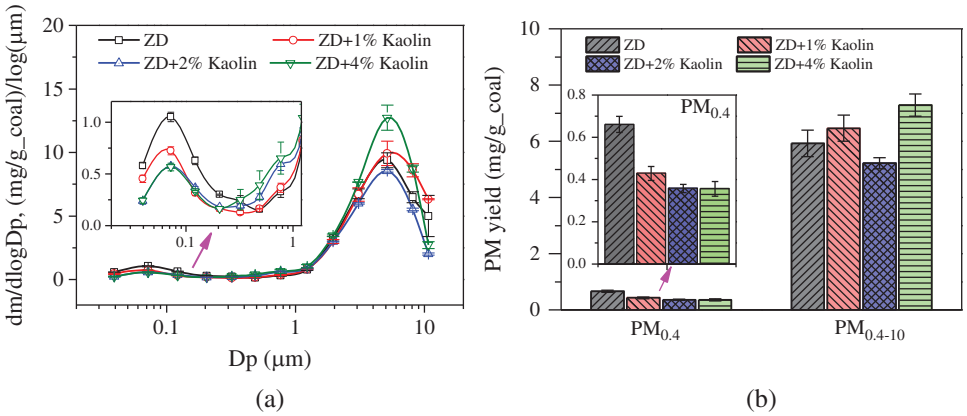

Figure 2: (a) PSDs before and after kaolin addition (b) PM yield before and after kaolin addition

3.2 Chemical Composition of PM_{10}

By comparing the chemical composition, how kaolin will affect the key elements can be clearly examined in detail.

Figs. 3a–3d present the size segregated composition of fine ash before and after kaolin addition. In the ZD coal (Fig. 3a) fine mode $PM_{0.4}$, in addition to the volatile Na_2O, K_2O and SO_3, it was mainly composed of MgO, CaO, and Fe_2O_3. The composition was similar to the submicron particles produced from American low rank coals [35] and Australia brown coal [33]. Such high content of refractory oxides was mainly attributed to the organically bound nature of Mg, Ca and Fe in the coal [33]. So they were more easy to decompose and vaporize than their mineral forms. While for the fragmentation mode $PM_{0.4\text{-}10}$, the composition was almost constant at each size. Where CaO was the major composition, accounting for more than 60 wt%. This was followed by MgO, Al_2O_3 and SiO_2, accounting for more than 30 wt%. The content of Fe_2O_3 was around 4 wt%. Nevertheless, the Na_2O content was very low in $PM_{0.4\text{-}10}$.

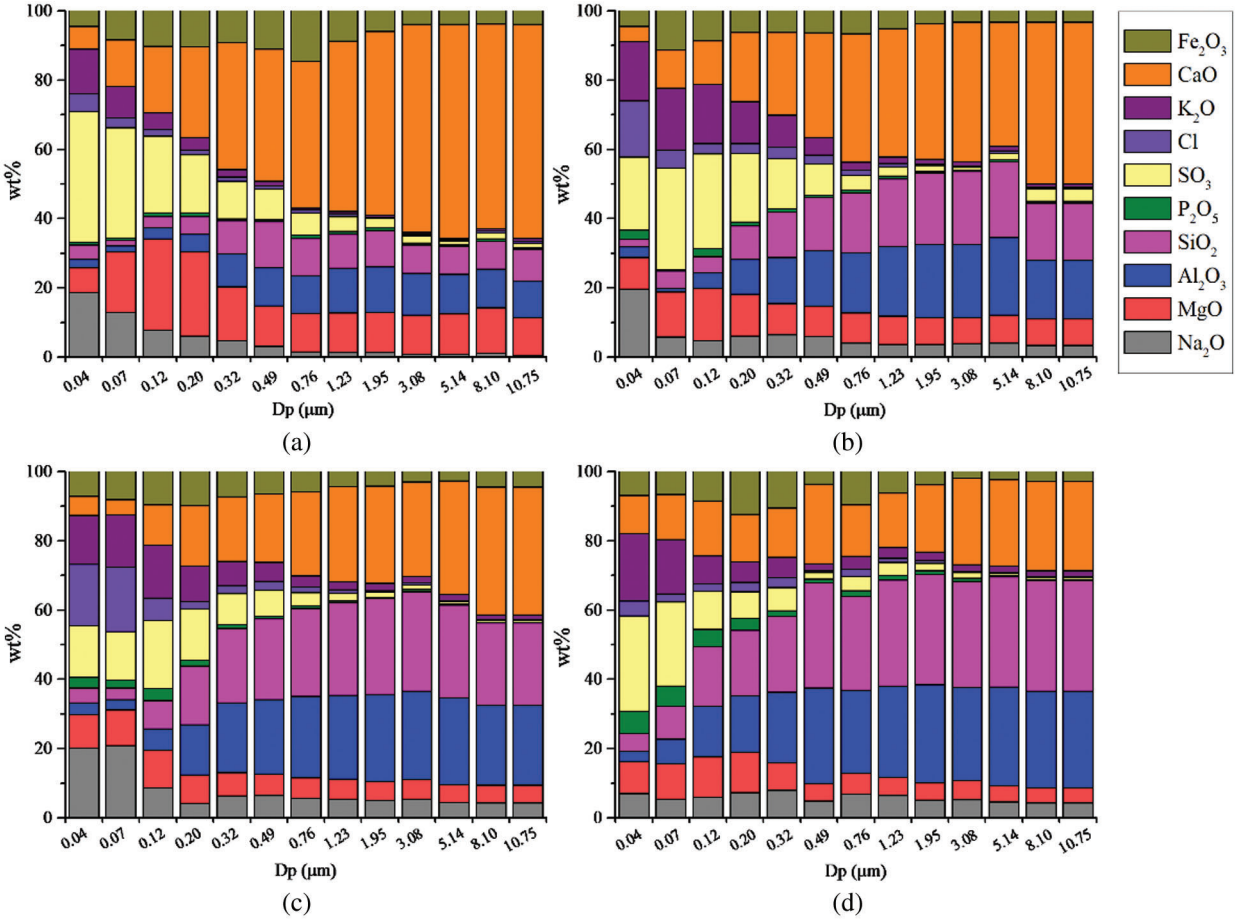

Figure 3: Composition of PM_{10} before and after kaolin addition (a) ZD (b) ZD + 1% Kaolin (c) ZD + 2% Kaolin (d) ZD + 4% Kaolin

By contrast, after kaolin addition, several changes can be observed. First, the content of SiO_2 and Al_2O_3 was significantly increased in the coarse mode $PM_{0.4\text{-}10}$, as well as in the fine mode $PM_{0.1\text{-}0.4}$, and gained with the increase of kaolin dosage. It suggests that kaolin participated in the formation of PM_{10}, which is reasonable since kaolin was fine (Fig. 1). Second, the content of Na_2O in the fine mode was decreased when 1% and 4% kaolin was introduced. Na_2O in the coarse mode was correspondingly increased. Third, and most importantly, the content of refractory CaO and MgO in both fine mode $PM_{0.4}$ and coarse mode $PM_{0.4\text{-}10}$ were significantly decreased and the content of refractory Fe_2O_3 was slightly decreased. It suggests that kaolin can also affect the transformation of Ca, Mg and Fe in the fine ash.

3.3 PSDs and Yields of Na, Ca, Mg and Fe in PM_{10}

Figs. 4a–4h present the mass-based PSD and the yield of Na_2O, CaO, MgO and Fe_2O_3 in PM_{10}. From Figs. 4a–4b, it can be seen that the mass of Na_2O in $PM_{0.4}$ was reduced by 50%, 50% and 75% at the kaolin dosage of 1%, 2% and 4%, respectively. And the mass of Na_2O in $PM_{0.4\text{-}10}$ was increased to 4~7 times of that in the ZD coal. It proved that kaolin indeed captured Na vapor during Zhundong coal combustion, inhibiting its nucleation and condensation into $PM_{0.4}$, and fixed it into $PM_{0.4\text{-}10}$.

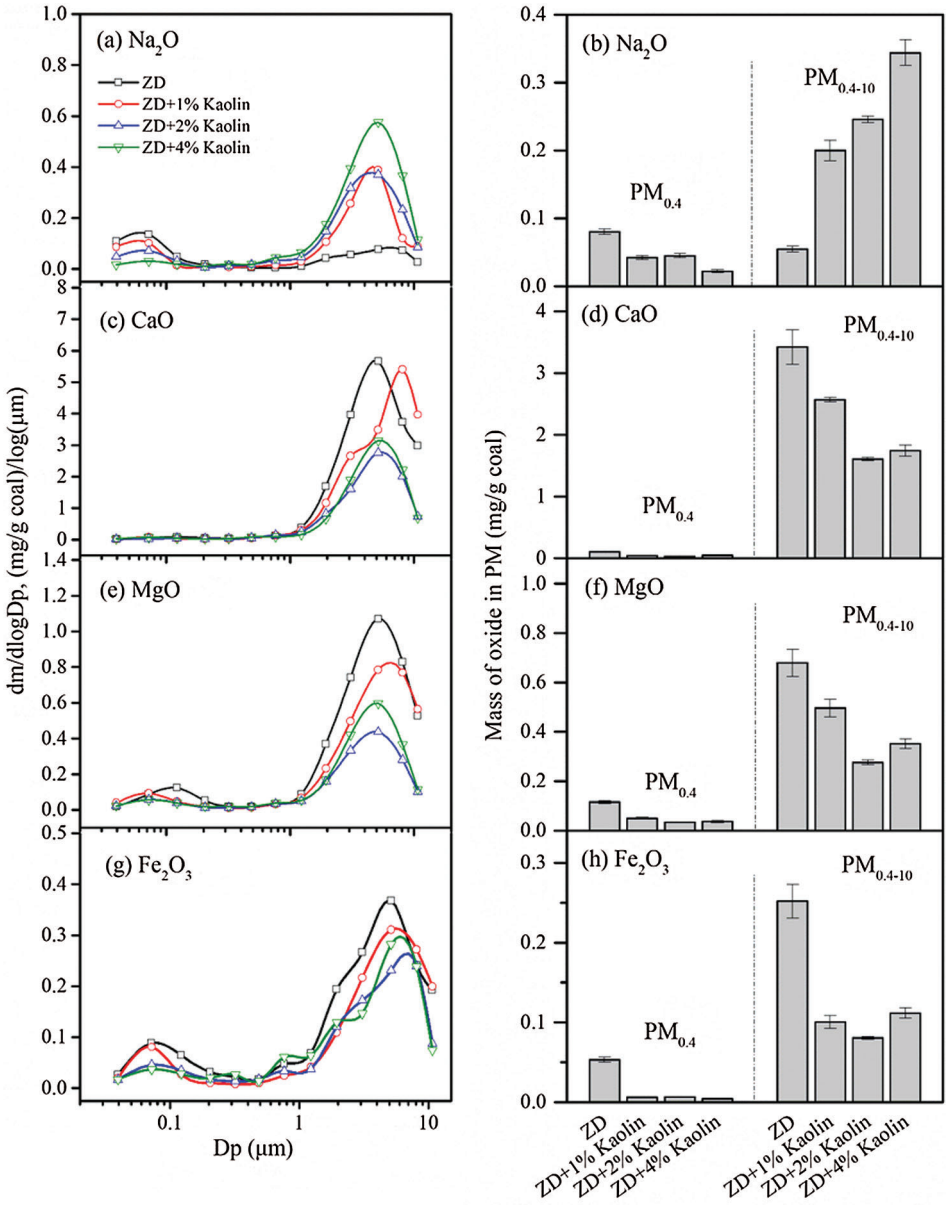

Figure 4: Mass distribution of Na, Ca and Mg in fine ash particles

Figs. 4c–4h show that CaO, MgO and Fe_2O_3 were mainly distributed in $PM_{0.4\text{-}10}$ during ZD coal combustion. This is because Ca, Mg and Fe were all refractory elements, so they formed $PM_{0.4\text{-}10}$ by coalescence and char fragmentation [34]. It was notable that they were all reduced significantly by kaolin addition. More than 50% of CaO, MgO and Fe_2O_3 were reduced in $PM_{0.4\text{-}10}$ at kaolin dosages of 2% and 4%. In addition, their mass in $PM_{0.4}$ was also decreased, and the amount was comparable with that of Na_2O in $PM_{0.4}$. These data demonstrated that, besides the capture of volatile Na, kaolin can also strongly capture refractory CaO, MgO and Fe_2O_3, affecting their transformation both in $PM_{0.4}$ and $PM_{0.4\text{-}10}$. This was a bit different from the results of Chen et al. [36], where only Na and K were significantly decreased in PM_1 after kaolin addition, while other elements were little changed. The difference may be caused by the different coal ash composition. The coal in Chen's work [36] was rich in SiO_2 and Al_2O_3, but

deficient in CaO and MgO. So the content of CaO and MgO in PM_1 may be low, and the mass changes after kaolin addition were insignificant.

To more clearly elucidate the effect of kaolin on the fine ash formation, the morphology and elemental mapping results of fine ash in the 11 stage (5 μm) of LPI before and after kaolin were presented in Figs. 5–7. Remarkable differences can be observed in both morphology and elemental mapping. The ZD fine ash (Fig. 5a) was mainly composed of sintered particles with irregular shape, in addition, several spherical particles can be observed. The elemental mapping results (Fig. 6) show that the sintered irregular particles were rich in Ca and Mg, together with some Al. While the spherical particles were mainly rich in Si-Na, Si-Al-Na, or Si-Al-Ca-Mg. After kaolin addition (Figs. 5b–5d), it is striking that the amount of sintered particles decreased significantly or even disappeared, which were replaced by a large number of smooth spherical particles. Elemental mapping results (Fig. 7) show that all these spherical particles were rich in both Si and Al, together with Ca/Mg and/or Na. The signal of Fe was weak due to its low content, it was seemed to disperse in all particles. These results directly demonstrated that kaolin additive participated in the fine ash formation by strongly scavenging Ca, Mg and Na from ZD coal, which finally formed melted Ca-Mg-Na containing spherical particles.

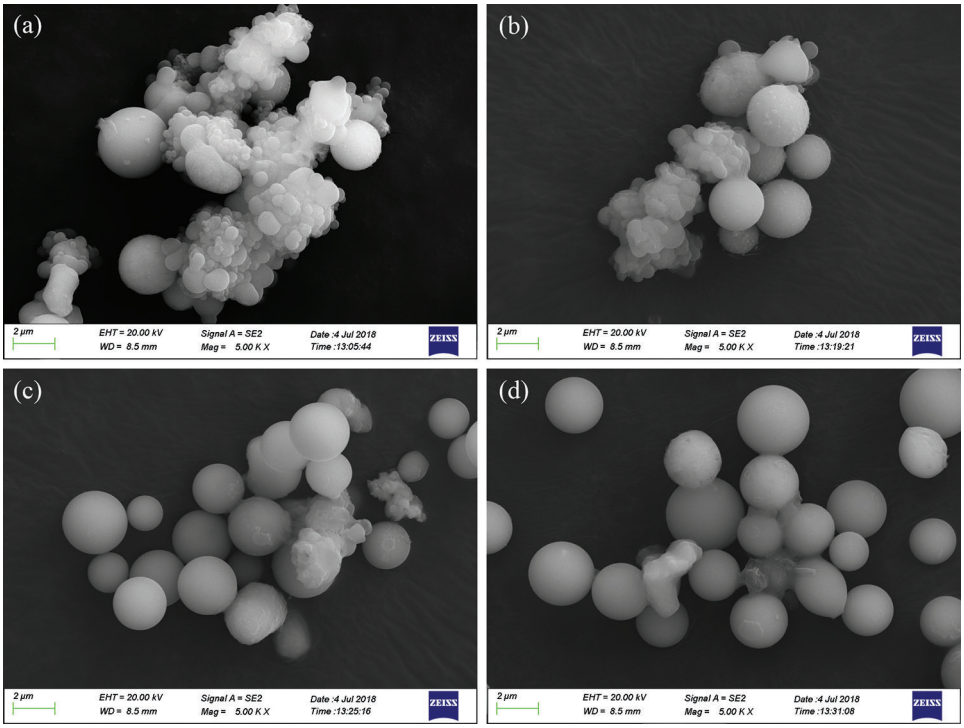

Figure 5: Morphology of coarse mode particles (a) ZD (b) ZD + 1% Kaolin (c) ZD + 2% Kaolin (d) ZD + 4% Kaolin

4 Discussion

The above results have suggested that, kaolin not only can capture Na, but also can strongly affect the transformation of refractory Ca, Mg and Fe in fine ash during Zhundong coal combustion. It has been well known that Na was captured by kaolin in terms of chemical adsorption between Na vapor and kaolin, which is vapor-solid interaction. In this way, Na vapor should diffuse from the surface of char particles to the surface of kaolin particles [37]. Then it was chemically adsorbed by kaolin. Note that, different from Na which was volatile, Ca, Mg and Fe were refractory elements, only very limited amounts of them can vaporize during

coal combustion [35]. So they can hardly diffuse to the surface of kaolin particles. Therefore, the reaction mechanism of Ca, Mg and Fe by kaolin should be different from that of Na.

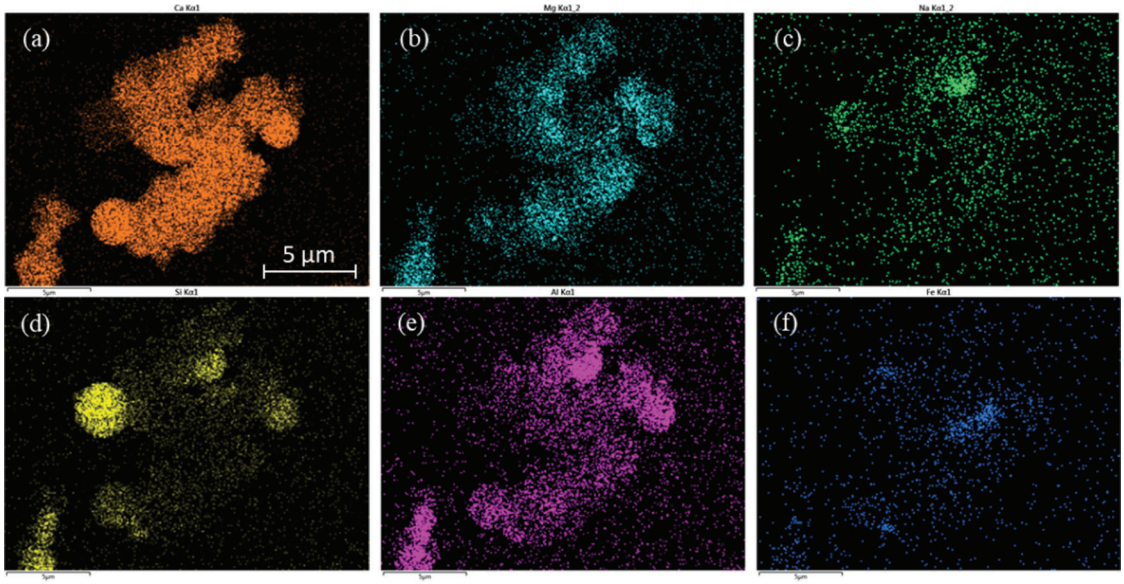

Figure 6: Elemental mapping of Na, Ca, Mg, Fe, Si, Al in $PM_{0.4\text{-}10}$ of ZD case (Fig. 5a) (a) Ca (b) Mg (c) Na (d) Si (e) Al (f) Fe

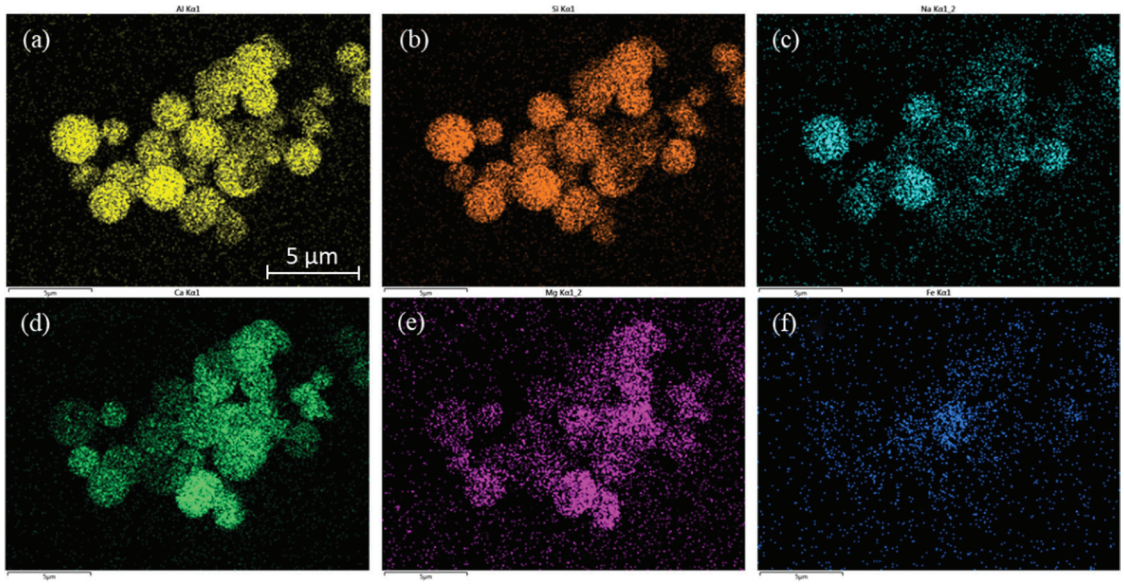

Figure 7: Elemental mapping of Na, Ca, Mg, Fe, Si, Al in $PM_{0.4\text{-}10}$ of ZD + 2% Kaolin case (Fig. 5c) (a) Al (b) Si (c) Na (d) Ca (e) Mg (f) Fe

Since kaolin can react with the Ca, Mg and Fe from coal particle, there should be contact between kaolin particles and coal particles. To gain insight into the dispersion state of kaolin among coal particles, the backscattered electro images (BSE) of ZD coal and ZD + 4% Kaolin were collected, as shown in Figs. 8a and 8b. BSE can distinguish different chemical phase by the gray-scale intensity. Particles with higher

atomic number will be brighter than particles with lower atomic number [38]. Thus the dispersion state of kaolin among coal particles can be clearly recognized. It can be found that the particles from ZD coal (Fig. 8a) were of the same grey level, meaning that ZD coal was mainly consists of carbon with rare excluded minerals. While there are many small and bright particles (marked in yellow) among the grey coal particles for the ZD + 4% Kaolin sample (Fig. 8b), some of them even attached on the coal surface. Composition analysis further confirmed that they were kaolin particles. Such close distance between coal and kaolin particles is expected to provide sufficient opportunities for their interactions during combustion.

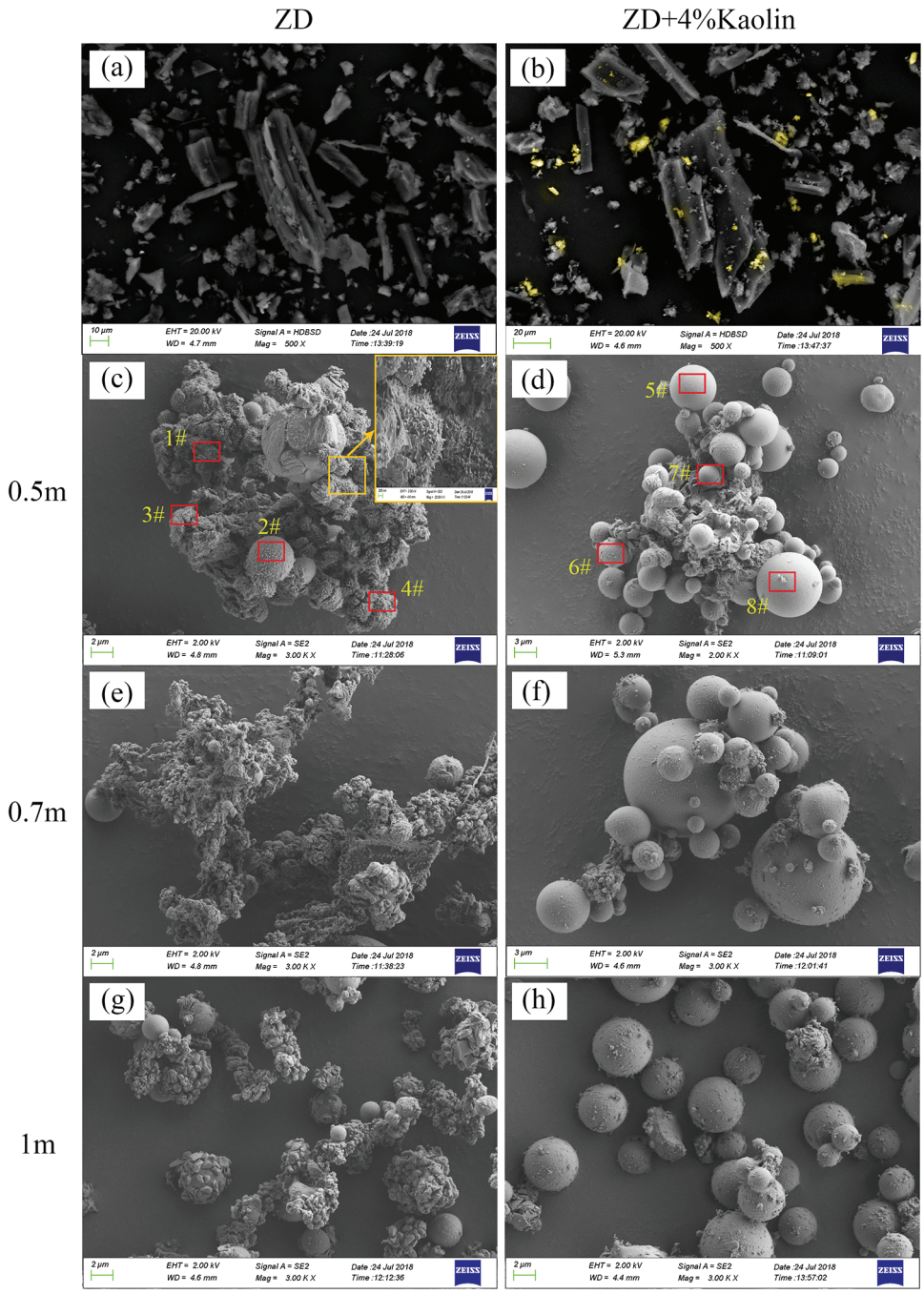

Figure 8: Fine ash formation process before and after kaolin addition

To reveal the evolution process of Ca, Mg and Fe into fine ashes after kaolin addition, the char/ash particles burnt at different positions of DTF were sampled and analyzed. Fig. 8c shows a partially burnt particle of ZD coal sampled at 0.5 m from the injector of DTF, where the resistance time was about 0.5 second. Clearly, the surface was covered by many ash grains with angular morphology. Composition analysis results (Tab. 3) show that these grains were all of high content of Ca, which ranged from 50 wt % to 93 wt%. Some grains were also of high Mg, such as 1#, 2# and 3#. Several spherical ashes (such as 2#) can also be observed, in which the contents of Si and Al were relatively higher. It suggested that during the early combustion stage of ZD coal, the organically bonded Ca and Mg were exposed to the char surface as the char edge receded due to carbon consumption. Despite most of them were organically bonded in the coal matrix [28], they did not seem to vaporize intensively to form fumes at this condition. On the contrary, they were mostly retained on the char surface. This can be explained by the high boiling point of CaO (2850°C) and MgO (3600°C) [28], which were much higher than the experimental temperature 1300°C. If quartz or kaolin grains were available, these fine Ca/Mg grains would also react with them and form melted Ca-Mg alumino-silicates [14]. Further combustion would lead to the fragmentation/breakup of char/ash particles, as shown in Fig. 8e. At this stage, char/ash particles were likely to breakup into several small pieces. The Ca-rich or Ca-Mg rich grains or Ca-Mg alumino-silicate droplets on each small piece would be most likely to form one or more sintered particle in the final ashing stage, as shown in Fig. 8g. It can be observed that most of the particles in Fig. 8g were in the size range of 1–10 μm, which is in agreement with the PSD results (Fig. 2a).

Table 3: Composition of selected particles (wt%)

	ZD				ZD + 4% Kaolin			
	1#	2#	3#	4#	5#	6#	7#	8#
Na	0.00	0.00	0.00	1.15	8.30	10.70	0.00	10.52
Mg	9.28	9.72	14.20	0.00	3.19	2.25	8.79	2.03
Ca	77.35	55.53	74.51	92.83	18.34	31.45	52.54	10.89
Si	2.60	14.80	0.00	1.04	33.71	24.60	17.65	36.04
Al	4.25	17.89	5.18	0.99	33.64	26.12	19.67	38.65
Fe	1.94	1.30	0.00	2.19	2.82	0.79	0.00	1.39
Others	4.58	0.76	6.11	1.80	0.00	4.09	1.35	0.48

When compared with the ZD coal case (Fig. 8c), it is interesting that the surface of the char in ZD + 4% Kaolin (Fig. 8d) was covered by many spherical particles, and their sizes range from 1 to 4 μm. Composition results (Tab. 3) show that they were all Na-Ca-Si-Al, Ca-Si-Al or Ca-Mg-Si-Al, indicating that they were resulted from the scavenging of Na, Ca and Mg by kaolin. And this process was very quickly, as the resistance time at this position was about 0.5 s. The following reasons should be responsible for this phenomenon: (1) The distance between kaolin and coal particles was very close, so once kaolin particle adhered to the coal surface, it could directly contact with the solid CaO/MgO grains that were exposed. This is a key step that contributes to the scavenging of Ca and Mg. (2) Na was likely to vaporize as NaOH vapor [13], which was very active and could react with kaolin quickly. (3) The Ca/Mg rich grains originated from the organically bonded Ca and Mg were also reported to be active [14]. Thus, as long as they contacted, kaolin would quickly react with them, forming melted Na/Ca/Mg containing aluminosilicates. As the char continued to burn, more Ca and Mg rich particles were exposed on the surface. The melted Na/Ca/Mg containing droplets that adhered on the char surface would continue to

embed them and react with them, and form new melted spherical particles. Meanwhile, char fragmentation was also expected, forming several small pieces. The small melted particles were likely to coalescence or agglomerate into bigger particles (Figs. 8f and 8h). Consequently, a large amount of Ca and Mg that presented in $PM_{0.4\text{-}10}$ during ZD coal combustion would be aggregated into bigger particles after kaolin addition. This explained why Ca and Mg were significantly decreased in $PM_{0.4\text{-}10}$ and $PM_{0.4}$ after kaolin addition (Figs. 4d and 4f). As for Fe, it was low in the ash (Tab. 3) and always co-existed with Ca/Mg in the same ash particle during ZD coal combustion, which was likely to be originated from the hydrochloric acid soluble Fe in the coal. So its trend was similar to that of Ca/Mg after kaolin addition, and was also significantly scavenged by kaolin. Thus, the mass of Fe_2O_3 in $PM_{0.4}$ and $PM_{0.4\text{-}10}$ was greatly reduced (Fig. 4h).

5 Conclusions

The effect of kaolin addition on the fine ash formation and the partitioning of Na, Ca, Mg and Fe in fine ash during Zhundong coal combustion was studied in a drop tube furnace at 1300°C. Kaolin dosages were 1, 2, 4 wt% of coal mass. Fine ashes were collected by a low pressure impactor and analyzed by SEM-EDS. It was found that, kaolin indeed strongly captured volatile Na during Zhundong coal combustion, which was expected. More importantly, kaolin additive can also strongly scavenge refractory Ca, Mg and Fe during Zhundong coal combustion. This significantly affected the fine ash formation by forming melted Na/Ca/Mg containing aluminosilicates, and finally resulted in the decrease of Ca, Mg and Fe in both fine mode $PM_{0.4}$ and coarse mode $PM_{0.4\text{-}10}$. The close distance between kaolin particles and coal particles that resulted from their physical mixing was the key factor that contributing to the scavenging of Ca, Mg, Fe by kaolin. Because it provided sufficient opportunities for the contact of solid kaolin and solid Ca, Mg grains derived from the coal.

Acknowledgement: Acknowledgements are also given for the supports from the Analytical and Testing Center at Huazhong University of Science and Technology.

Funding Statement: This research was funded by the National Key Research and Development Program of China (No. 2016YFB0600601) and National Natural Science Foundation of China (Nos. 51676075 and 51520105008).

Conflicts of Interest: The authors declare that they have no conflicts of interest to report regarding the present study.

References

1. Benson, S. A., Sondreal, E. A. (1998). Impact of low-rank coal properties on advanced power systems. *Fuel Processing Technology, 56(1–2),* 129–142. DOI 10.1016/S0378-3820(98)00059-9.
2. Sondreal, E. A., Tufte, P. H., Beckering, W. (1977). Ash fouling in the combustion of low rank western U.S. Coals. *Combustion Science and Technology, 16(3–6),* 95–110. DOI 10.1080/00102207708946797.
3. Kalmanovitch, D., Zygarlicke, C., Steadman, E., Benson, S. (1989). Deposition of Beulah ash in a drop-tube furnace under slagging conditions. *American Chemical Society, Division of Fuel Chemistry, Preprints, 34,* 318–329.
4. McCollor, D. P., Zygarlicke, C. J., Allan, S. E., Benson, S. A. (1993). Ash deposit initiation in a simulated fouling regime. *Energy & Fuels, 7(6),* 761–767. DOI 10.1021/ef00042a010.
5. Bryers, R. W. (1996). Fireside slagging, fouling, and high-temperature corrosion of heat-transfer surface due to impurities in steam-raising fuels. *Progress in Energy and Combustion Science, 22(1),* 29–120. DOI 10.1016/0360-1285(95)00012-7.
6. Dai, B. Q., Low, F., de Girolamo, A., Wu, X. J., Zhang, L. A. (2013). Characteristics of ash deposits in a pulverized lignite coal-fired boiler and the mass flow of major ash-forming inorganic elements. *Energy & Fuels, 27(10),* 6198–6211. DOI 10.1021/ef400930e.

7. Li, G. D., Li, S. Q., Huang, Q., Yao, Q. (2015). Fine particulate formation and ash deposition during pulverized coal combustion of high-sodium lignite in a down-fired furnace. *Fuel, 143,* 430–437. DOI 10.1016/j.fuel.2014.11.067.
8. Wang, X. B., Xu, Z. X., Wei, B., Zhang, L., Tan, H. Z. et al. (2015). The ash deposition mechanism in boilers burning Zhundong coal with high contents of sodium and calcium: A study from ash evaporating to condensing. *Applied Thermal Engineering, 80,* 150–159. DOI 10.1016/j.applthermaleng.2015.01.051.
9. Ruan, R. H., Tan, H. Z., Wang, X. B., Li, Y., Li, S. S. et al. (2018). Characteristics of fine particulate matter formation during combustion of lignite riched in AAEM (alkali and alkaline earth metals) and sulfur. *Fuel, 211,* 206–213. DOI 10.1016/j.fuel.2017.08.114.
10. Pope III, C. A., Dockery, D. W. (2012). Health effects of fine particulate air pollution: Lines that connect. *Journal of the Air & Waste Management Association, 56(6),* 709–742. DOI 10.1080/10473289.2006.10464485.
11. Damle, A., Ensor, D., Ranade, M. (2008). Coal combustion aerosol formation mechanisms: A review. *Aerosol Science and Technology, 1(1),* 119–133. DOI 10.1080/02786828208958582.
12. Lighty, J. S., Veranth, J. M., Sarofim, A. F. (2011). Combustion aerosols: Factors governing their size and composition and implications to human health. *Journal of the Air & Waste Management Association, 50(9),* 1565–1618. DOI 10.1080/10473289.2000.10464197.
13. Wibberley, L. J., Wall, T. F. (1982). Alkali-ash reactions and deposit formation in pulverized-coal-fired boilers: The thermodynamic aspects involving silica, sodium, sulphur and chlorine. *Fuel, 61(1),* 87–92. DOI 10.1016/0016-2361(82)90298-8.
14. Huffman, G., Huggins, F., Shah, N., Shah, A. (1990). Behavior of basic elements during coal combustion. *Progress in Energy and Combustion Science, 16(4),* 243–251. DOI 10.1016/0360-1285(90)90033-Y.
15. Miller, S. F., Schobert, H. H. (1994). Effect of the occurrence and modes of incorporation of alkalis, alkaline earth elements, and sulfur on ash formation in pilot-scale combustion of Beulah pulverized coal and coal-water slurry fuel. *Energy & Fuels, 8(6),* 1208–1216. DOI 10.1021/ef00048a007.
16. Vuthaluru, H. B., Vleeskens, J. M., Wall, T. F. (1998). Reducing fouling from brown coals by sodium-binding additives. *Fuel Processing Technology, 55(2),* 161–173. DOI 10.1016/S0378-3820(98)00042-3.
17. Kyi, S., Chadwick, B. L. (1999). Screening of potential mineral additives for use as fouling preventatives in Victorian brown coal combustion. *Fuel, 78(7),* 845–855. DOI 10.1016/S0016-2361(98)00205-1.
18. Li, C. Z., Sathe, C., Kershaw, J. R., Pang, Y. (2000). Fates and roles of alkali and alkaline earth metals during the pyrolysis of a Victorian brown coal. *Fuel, 79(3–4),* 427–438. DOI 10.1016/S0016-2361(99)00178-7.
19. Punjak, W. A., Uberoi, M., Shadman, F. (1989). Control of ash deposition through the high temperature adsorption of alkali vapors on solid sorbents. *ACS Division of Fuel Chemistry,* preprints of papers presented at the ACS National Meeting in Dallas, Texas.
20. Takuwa, T., Naruse, I. (2007). Emission control of sodium compounds and their formation mechanisms during coal combustion. *Proceedings of the Combustion Institute, 31(2),* 2863–2870.l. DOI 10.1016/j.proci.2006.07.170.
21. Wei, B., Wang, X. X., Tan, H. Z., Zhang, L. M., Wang, Y. B. et al. (2016). Effect of silicon–aluminum additives on ash fusion and ash mineral conversion of Xinjiang high-sodium coal. *Fuel, 181,* 1224–1229. DOI 10.1016/j.fuel.2016.02.072.
22. Xu, Y. S., Liu, X. W., Wang, H., Zeng, X. P., Zhang, Y. F. et al. (2018). Influences of In-Furnace Kaolin addition on the formation and emission characteristics of $PM_{2.5}$ in a 1000 MW coal-fired power station. *Environmental Science and Technology, 52(15),* 8718–8724. DOI 10.1021/acs.est.8b02251.
23. Takuwa, T., Mkilaha, I. S. N., Naruse, I. (2006). Mechanisms of fine particulates formation with alkali metal compounds during coal combustion. *Fuel, 85(5–6),* 671–678. DOI 10.1016/j.fuel.2005.08.043.
24. Chen, J., Yao, H., Zhang, P. A., Xiao, L., Luo, G. et al. (2011). Control of PM1 by kaolin or limestone during O_2/CO_2 pulverized coal combustion. *Proceedings of the Combustion Institute, 33(2),* 2837–2843. DOI 10.1016/j.proci.2010.06.158.
25. Punjak, W. A., Uberoi, M., Shadman, F. (1989). Control of ash deposition through the high temperature adsorption of alkali vapors on solid sorbents. In: *Symposium on Ash Deposition, 197th Annual Meeting of the American Chemical Society.* Dallas, TX: University of Arizona.

26. Logan, R. G., Richards, G. A., Meyer, C. T., Anderson, R. J. (1990). A study of techniques for reducing ash deposition in coal-fired gas turbines. *Progress in Energy and Combustion Science, 16(4),* 221–233. DOI 10.1016/0360-1285(90)90031-W.
27. Ohman, M., Nordin, A. (2000). The role of kaolin in prevention of bed agglomeration during fluidized bed combustion of biomass fuels. *Energy & Fuels, 14(3),* 618–624. DOI 10.1021/ef990198c.
28. Zeng, X. P., Yu, D. X., Liu, F. Q., Fan, B., Wen, C. et al. (2018). Scavenging of refractory elements (Ca, Mg, Fe) by kaolin during low rank coal combustion. *Fuel, 223,* 198–210. DOI 10.1016/j.fuel.2018.03.033.
29. Yu, D. X., Xu, M. H., Zhang, L. A., Yao, H., Wang, Q. Y. et al. (2007). Computer-controlled scanning electron microscopy (CCSEM) investigation on the heterogeneous nature of mineral matter in six typical Chinese coals. *Energy & Fuels, 21(2),* 468–476. DOI 10.1021/ef060419w.
30. Zygarlicke, C., Steadman, E., Benson, S. (1990). Studies of transformations of inorganic constituents in a Texas lignite during combustion. *Progress in Energy and Combustion Science, 16(4),* 195–204. DOI 10.1016/0360-1285(90)90028-2.
31. Yu, D. X., Zhao, L. A., Zhang, Z. Y., Wen, C., Xu, M. H. et al. (2012). Iron transformation and ash fusibility during coal combustion in air and O_2/CO_2 medium. *Energy & Fuels, 26(6),* 3150–3155. DOI 10.1021/ef201786v.
32. Lipsky, E., Stanier, C. O., Pandis, S. N., Robinson, A. L. (2002). Effects of sampling conditions on the size distribution of fine particulate matter emitted from a pilot-scale pulverized-coal combustor. *Energy & Fuels, 16(2),* 302–310. DOI 10.1021/ef0102014.
33. Gao, X. P., Rahim, M. U., Chen, X. X., Wu, H. W. (2014). Significant contribution of organically-bound Mg, Ca, and Fe to inorganic PM_{10} emission during the combustion of pulverized Victorian brown coal. *Fuel, 117,* 825–832. DOI 10.1016/j.fuel.2013.09.056.
34. Xu, M. H., Yu, D. X., Yao, H., Liu, X. W., Qiao, Y. (2011). Coal combustion-generated aerosols: Formation and properties. *Proceedings of the Combustion Institute, 33(1),* 1681–1697. DOI 10.1016/j.proci.2010.09.014.
35. Quann, R. J., Sarofim, A. F. (1982). Vaporization of refractory oxides during pulverized coal combustion. *Symposium (International) on Combustion, 19(1),* 1429–1440. DOI 10.1016/S0082-0784(82)80320-2.
36. Chen, J. A., Yao, H., Zhang, P. A., Xiao, L., Luo, G. Q. et al. (2011). Control of PM_1 by kaolin or limestone during O_2/CO_2 pulverized coal combustion. *Proceedings of the Combustion Institute, 33(2),* 2837–2843. DOI 10.1016/j.proci.2010.06.158.
37. Gale, T. K., Wendt, J. O. (2003). Mechanisms and models describing sodium and lead scavenging by a kaolinite aerosol at high temperatures. *Aerosol Science and Technology, 37(11),* 865–876. DOI 10.1080/02786820300929.
38. Kutchko, B., Kim, A. (2006). Fly ash characterization by SEM-EDS. *Fuel, 85(17–18),* 2537–2544. DOI 10.1016/j.fuel.2006.05.016.